IEEE Access
Multidisciplinary | Rapid Review | Open Access Journal

Received January 4, 2021, accepted January 11, 2021, date of publication January 18, 2021, date of current version February 2, 2021.

*Digital Object Identifier 10.1109/ACCESS.2021.3052057*

# A New Detecting Method for Underwater Acoustic Weak Signal Based on Differential Double Coupling Oscillator

**GUOHUI LI, JIUYANG CUI, AND HONG YANG**
School of Electronic Engineering, Xi'an University of Posts and Telecommunications, Xi'an 710121, China
Corresponding authors: Guohui Li (lghcd@163.com) and Hong Yang (uestcyhong@163.com)

This work was supported by the National Natural Science Foundation of China under Grant 51709228.

**ABSTRACT** For weak signal detection with known frequency, based on the double coupling Duffing oscillator method, a differential double coupling Duffing oscillator and Van der Pol-Duffing oscillator detection method is proposed. Its feasibility is verified by sinusoidal analog signal. It has intuitive detection effect and high sensitivity, and can detect weak signal with lower signal-to-noise ratio (SNR). For underwater acoustic weak signal detection with unknown frequency, based on the above proposed method, a differential double coupling Duffing oscillator and Van der Pol-Duffing oscillator variable step-size detection method is proposed. Compared with the existing double coupling Duffing oscillator variable step-size method and differential double Duffing oscillator variable step-size method, its SNR threshold is respectively reduced by 6.02dB and 2.28dB. The lowest average error rate of frequency estimation in multiple sinusoidal analog signal detection under Gaussian white noise, Gaussian color noise and Rayleigh distribution noise is 0.423%. Its detection effect is verified in the detection of measured underwater acoustic signals from the website http://atlanttic.uvigo.es/underwaternoise/. The results show that it has good detection performance. It provides a new detecting method for underwater acoustic weak signal. In the future, it can be applied to detect weak periodic signal such as square wave and general periodic signal with unknown frequency.

**INDEX TERMS** Weak signal detection, difference, double coupling, Duffing oscillator, underwater acoustic weak signal.

## I. INTRODUCTION

Weak signal detection refers to the detection of parameters such as phase, amplitude and frequency of weak signal submerged in strong noise background. It is widely used in communication signal, underwater acoustic signal, fault diagnosis and radar detection [1]–[6]. In weak signal detection, adaptive line spectrum enhancer [7], wavelet detection [8], [9], high-order statistics detection [10]–[14], neural network detection [15]–[17], stochastic resonance method [18] and so on are commonly used to enhance signal and suppress background noise on the basis of linear theory. However, when the marine environment is more complex, spectrum analysis and stochastic system theory will have great limitations. Conventional weak signal detection method cannot realize the detection of low signal-to-noise ratio (SNR) underwater acoustic signal. In complex ocean environment, the detection of underwater acoustic signal has always been a difficult problem perplexing the underwater acoustic community, and it is also a key problem that needs to be solved urgently for quiet underwater target detection. Especially for the detection of underwater acoustic signal with unknown frequency, it is urgent to propose effective detection method.

The principle of chaotic oscillator detection in underwater acoustic weak signal is based on the sensitivity of chaotic oscillator to periodic signal with low SNR and immunity to noise. The traditional underwater acoustic weak signal detection method uses a single chaotic oscillator to complete the detection, mainly including amplitude variation coefficient method [19], parameter suppression method [20], rapid transverse filtering ALE method [21], and so on. However, the SNR threshold of the single chaotic oscillator detection method is too high, the detection bandwidth is limited, some useful signals will be lost, and the parameter problem of the signal to be detected with unknown frequency is not solved. To solve this problem, some scholars have proposed a method

The associate editor coordinating the review of this manuscript and approving it for publication was Prakasam Periasamy.

of coupling chaotic oscillator and double chaotic oscillator. Coupling chaotic oscillator is to couple two oscillators through linear restoring force, which improves the sensitivity of the system to periodic signal with low SNR and the ability to suppress noise compared with single chaotic oscillator. Double coupling Duffing oscillator method [22], Duffing oscillator and Van der Pol-Duffing oscillator coupling method [23], double coupling Van der Pol-Duffing oscillator method [24], bidirectional ring coupling Duffing oscillator transient synchronous mutation method [25] and so on are proposed. These methods improve the detection SNR to some extent, and increase the speed and accuracy of threshold solution. Double chaotic oscillators form output phase difference between the two oscillators through difference, which is convenient to eliminate common-mode interference. The current state is judged by phase diagram. Differential double Duffing oscillator detection method [26], [27], differential double oscillator array method [28], two-coupled differential Van der Pol-Duffing oscillator method [29] and so on are proposed for ship-radiated noise signal detection. Good detection effect is achieved and calculation amount is reduced, but the detection performance of double Duffing oscillator still needs to be improved. In terms of optimizing oscillator detection performance, some methods can reduce the SNR threshold to some extent, such as differential double Duffing oscillator detection method [30], [31], variable scale-convex-peak method [32], inverse phase change chaotic detection method, combining high-order cumulant and Duffing oscillator [33], double coupling Duffing oscillator detection method [34], [35], Duffing oscillator detection method [36] which can determine bifurcation diagram and dichotomy of the critical threshold of the signal to be detected, and coupling double Duffing oscillator method [37] which applies restoring force and damping to force. However, these methods still do not solve the problem of parameter estimation for unknown frequency signal. When detecting unknown frequency signal, some methods are proposed such as Lyapunov exponents used to determine detection threshold method [38], drive-response method to construct synchronous detection system method [39], oscillator array method combined with genetic algorithm [40], intermittent chaotic oscillator array method [41], inverse phase change scaling method [42], [43] and adaptive step-size intermittent chaotic method [44]. These methods solve the parameter estimation problem of unknown frequency signal to some extent, but they still have the problem of high SNR threshold.

Aiming at the periodic signal with known frequency, combining the idea of oscillator coefficient difference and oscillator coupling, a differential double coupling Duffing oscillator and Van der Pol-Duffing oscillator detection method, named the proposed method 1, is proposed. It is used to detect sinusoidal analog signal. In practical work, the frequency of most signals to be measured is unknown. There are also many situations in the frequency distribution of signals. The periodic signal detection by chaotic oscillator is mainly based on the change of the system from critical chaotic state to large-scale periodic state, but this method can only be used to detect the condition that the frequency of the signal to be measured is known, and it is unavailable when the frequency of the signal to be measured is unknown. Aiming at underwater acoustic weak signal detection with unknown frequency, based on the proposed method 1, combining with intermittent chaos theory, a differential double coupling Duffing oscillator and Van der Pol-Duffing oscillator variable step-size detection method, named the proposed method 2, is proposed. It is used to detect multiple sinusoidal analog signals under Gaussian white noise, Gaussian color noise, Rayleigh distribution noise and measured underwater acoustic signals. The proposed method 2 combines the theoretical ideas of intermittent chaos and variable step size method, so the signal frequency estimation results will be more accurate.

The specific content of this paper is organized as follows. In Section 2, differential double coupling Duffing oscillator and Van der Pol-Duffing oscillator detection method is proposed. In Section 3, differential double coupling Duffing oscillator and Van der Pol-Duffing oscillator variable step-size detection method is proposed. The simulation results of three kinds of analog signals are given. In Section 4, the detection results of double coupling Duffing oscillator and Van der Pol-Duffing oscillator variable step-size detection method, differential double Duffing oscillator variable step-size detection method and differential double coupling Duffing oscillator and Van der Pol-Duffing oscillator variable step-size detection method for measured ship-radiated noise signal are given. In Section 5, 6, the discussion and conclusion are given.

## II. DIFFERENTIAL DOUBLE COUPLING DUFFING OSCILLATOR AND VAN DER POL-DUFFING OSCILLATOR DETECTION METHOD

### A. DUFFING OSCILLATOR DETECTION METHOD

In the weak signal detection of chaotic system, the Holmes Duffing chaotic oscillator with nonlinear dynamic characteristics is usually selected [45]. The dynamic equation form of a single Holmes Duffing oscillator is as follows:

$$x'' + kx' + ax^3 - bx = \gamma \cos \omega t \tag{1}$$

where, $x$ is a chaotic system variable, $k$ is damping coefficient, $ax^3 - bx$ is the nonlinear restoring force coefficient, $\gamma$ is the amplitude of periodic policy force, $\omega$ is the angular frequency of periodic power. $\gamma \cos \omega t$ is the driving force of periodic policy. When $\gamma$ of a nonlinear system with complex dynamics changes, the phase diagram of the system will show the states of attractor, homoclinic orbit, period doubling bifurcation, chaos, critical chaos and large-scale period in sequence.

Under the condition of no noise, the large-scale periodic state and chaotic state of the chaotic oscillator detection system are smooth, but there is more or less noise in the actual signal. When the color noise $n(t)$ with a mean value of zero is input into the chaotic system, its influence on the detection performance of the oscillator is analyzed. The

Holmes Duffing oscillator subsystem equation is written as:

$$\begin{cases} x' = y \\ y' = -ky + x - x^3 + \gamma \cos \omega t + n(t) \end{cases} \tag{2}$$

where, $n(t)$ is colored noise, and $E\{n(t)\} = 0$. Assuming that $\Delta x(t)$ is the disturbance of noise to $x(t)$, the oscillator equation is changed to:

$$\begin{aligned} &(x'' + \Delta x'') + k(x' + \Delta x') - (x + \Delta x) + (x + \Delta x)^3 \\ &\quad = \gamma \cos \omega t + n(t) \end{aligned} \tag{3}$$

Let $a = 1$ and $b = 1$ in Equation (1), and get:

$$x'' + kx' + x^3 - x = \gamma \cos \omega t \tag{4}$$

Subtract Equation (4) from Equation (3). Because the value of $\Delta x$ is very small, the higher order term of $\Delta x$ can be omitted. It is obtained as follows:

$$\Delta x'' + k\Delta x' - \Delta x + 3x^2\Delta x + 3x\Delta x^2 + \Delta x^3 = n(t) \tag{5}$$

Let $b(t) = 1 - 3x^2$, and get:

$$\Delta x'' + k\Delta x' - b(t)\Delta x = n(t) \tag{6}$$

Change Equation (5) into vector equation form:

$$\boldsymbol{X}'(t) = \boldsymbol{H}(t)\boldsymbol{X}(t) + \boldsymbol{N}(t) \tag{7}$$

among them

$$\boldsymbol{X}(t) = \begin{bmatrix} \Delta x(t) \\ \Delta x'(t) \end{bmatrix}, \boldsymbol{H}(t) = \begin{bmatrix} 0 & 1 \\ b(t) & -k \end{bmatrix}, \boldsymbol{N}(t) = \begin{bmatrix} 0 \\ n(t) \end{bmatrix},$$

and

$$\boldsymbol{X}(t) = \boldsymbol{\Phi}(t, t_0)\boldsymbol{X}_0 + \int_{t_0}^{t} \boldsymbol{\Phi}(t, u)\boldsymbol{N}(u)du \tag{8}$$

where, $\boldsymbol{\Phi}$ is the state transition matrix of the system, and $\boldsymbol{\Phi}(t, t_0)\boldsymbol{X}_0$ is the transient solution, which will quickly decay to zero with time. So ignoring the solution, we get:

$$\boldsymbol{X}(t) = \int_{t_0}^{t} \boldsymbol{\Phi}(t, u)\boldsymbol{N}(u)du \tag{9}$$

The mean value of $\boldsymbol{X}(t)$ is:

$$E\{\boldsymbol{X}(t)\} = \int_{t_0}^{t} \boldsymbol{\Phi}(t, u)E\{\boldsymbol{N}(u)\}du = 0 \tag{10}$$

The mean square deviation of $\boldsymbol{X}(t)$ is obtained:

$$D\{\boldsymbol{X}(t)\} = E\left\{\boldsymbol{X}(t)\boldsymbol{X}^T(t)\right\} = \Gamma_{XX}(t, t) \tag{11}$$

where $\Gamma_{XX}(t, t)$ is the autocorrelation function of noise.

Because $\Gamma_{XX}(t, t) = \Gamma_{XX}(t + nT, t + nT)$, this process is a cyclic equilibrium process, which proves that noise has no fundamental influence on the phase trajectory of Duffing oscillator, but only coarsens the periphery of the phase trajectory of the oscillator, without affecting its detection performance. Noise distribution is not involved, so this conclusion is also applied to zero-mean white noise and color noise.

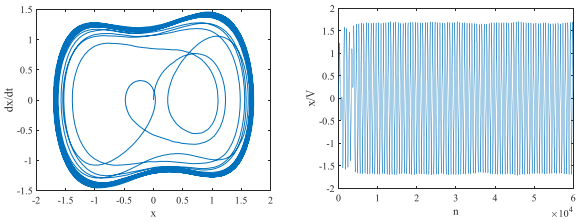


(a) Phase diagram (b) Timing diagram

**FIGURE 1.** System critical chaotic state and timing diagram.

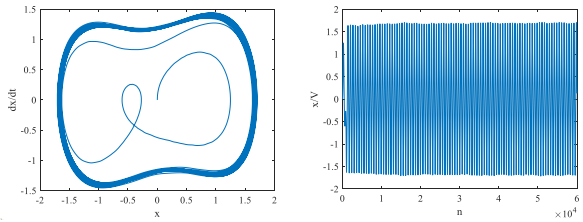


(a) Phase diagram (b) Timing diagram

**FIGURE 2.** Detection phase and timing diagram when $A = 0.009$.

When a signal is input into a chaotic system, the dynamic equation is:

$$x'' + kx'' + ax^3 - bx = \gamma \cos \omega t + A \cos(\omega_1 t) + n(t) \tag{12}$$

where $A$ is the signal amplitude, $n(t)$ is Gaussian white noise with variance $\delta^2$.

The Duffing chaotic oscillator is used to detect weak signals. Here, $a$ in Equation (12) is taken as 1, $b$ is taken as 1, and coefficient $k$ is taken as 0.5, sampling frequency is 100Hz. By adjusting the appropriate $\gamma$ value, the chaotic system is in a critical chaotic state shown in Figure 1, where $\gamma$ is adjusted to be 0.826.

At this time, if the frequency of the input signal is equal to the built-in power frequency of the chaotic system and the input signal meets the SNR threshold of the detection system, the phase diagram of the system will change from the critical chaotic state to the large-scale periodic state, which means that the input signal is successfully detected. If the above conditions are not met, the system phase diagram will appear chaos. For example, let $\omega$ take 1rad/s and $n(t)$ be Gaussian white noise with variance $\delta^2$ =0.01, sampling frequency is 100Hz. Here, $A\cos(\omega_1 t) + n(t)$ in Equation (12) is taken as the signal to be measured, and the signal amplitude is adjusted and then detected by a single Duffing vibrator detection system. The detection results are shown in Figure 2 and Figure 3.

When $A = 0.009$, the detection phase diagram of the system shows that the detection system is in a large-scale periodic state, and the signal to be detected is successfully detected. When $A = 0.008$, the system state does not change, and the phase diagram shows that the detection system is in a chaotic state and cannot detect the signal to be detected. After determining the amplitude $A$ of the periodic signal and the variance $\delta^2$ of Gaussian white noise, the SNR of the detection system can be calculated according to the calculation for-

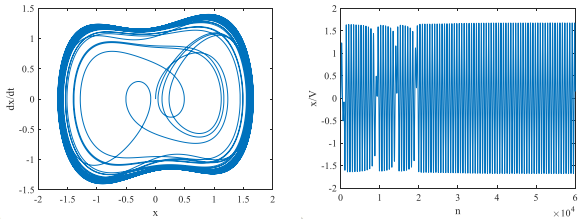

(a) Phase diagram (b) Timing diagram

**FIGURE 3.** Detection phase and timing diagram when $A = 0.008$.

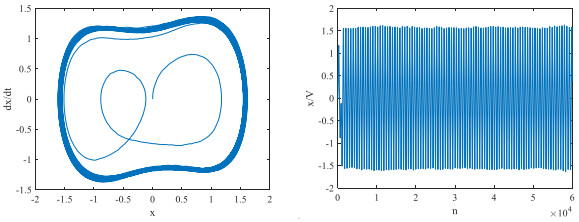

(a) Phase diagram (b) Timing diagram

**FIGURE 4.** Detection phase and timing diagram when $A = 0.0025$.

mula:

$$SNR = 10 \cdot \lg \frac{A^2}{2 \cdot \delta^2} \tag{13}$$

According to Equation (13), the lowest detection SNR of the system at this time can be calculated to be −23.926dB.

### B. DOUBLE COUPLING DUFFING OSCILLATOR AND VAN DER POL-DUFFING OSCILLATOR DETECTION METHOD

Van der Pol-Duffing oscillator [46] is widely used as an oscillator to describe oscillation in the fields of physics, biology and mechanics. Its dynamic equation is as follows:

$$x'' + \beta(x^2 - 1)x' + kx = \gamma \cos(\omega t) \tag{14}$$

where, $\beta$ is the damping coefficient, $k$ is the stiffness coefficient, $\gamma$ and $\omega$ are the amplitude and frequency of periodic poling force respectively. Because Duffing oscillator and Van der Pol-Duffing oscillator have immunity to noise and sensitivity to initial state, weak signal can be effectively detected. Coupling Duffing oscillator and Van der Pol-Duffing oscillator is an improved method based on the detection method of single Duffing oscillator. The two chaotic oscillators are coupled together through linear coupling to improve the sensitivity of the system to initial value and the anti-interference ability to noise. The equation for coupling Duffing oscillator and Van der Pol-Duffing oscillator is:

$$\begin{cases} x'' + kx' + ax^3 - bx + d(x - y) = \gamma \cos \omega t \\ y'' + \beta(1 + y^2)y' + y + d(y - x) = \gamma \cos \omega t \end{cases} \tag{15}$$

The coupling Duffing oscillator and Van der Pol-Duffing oscillator model belong to the same chaotic system model as the single Duffing oscillator model, and also show the system states of attractor, homoclinic orbit, period doubling bifurcation, chaos, critical chaos and large-scale period with the increase of the amplitude of the built-in poling force. The value of $\gamma$ here is adjusted to 0.7885, which makes the coupling double oscillator subsystem of Equation (15) in a system state of critical chaos. When the coupling Duffing oscillator and the Van der Pol-Duffing oscillator subsystem are used to detect weak periodic signals, the same input signal to be detected is given to the two oscillators, and the system equation at this time is:

To verify the improvement of anti-noise capability of the coupling Duffing oscillator and the Van der Pol-Duffing oscillator detection method compared with the single Duffing oscillator method, $\omega$ is taken as 1rad/s, $n(t)$ is Gaussian white noise with variance $\delta^2$ =0.01, $k$ is 0.5, $\gamma$ is 0.7885, $a$ is 1, $b$ is 1, sampling frequency is 100Hz, and coupling coefficient $d$ is taken as 0.2. The detection result after adjusting the signal amplitude $A$ is shown in Figure 4.

When the signal amplitude $A$ is 0.0025, the detection system changes from a critical chaotic state to a large-scale periodic state, and the signal can be detected. According to Equation (13), the lowest detection SNR of the coupling Duffing oscillator and Van der Pol-Duffing oscillator subsystem at this time can be calculated to be −35.05dB. At this time, the SNR threshold of weak periodic signal detected by the coupling Duffing oscillator and the Van der Pol-Duffing oscillator subsystem is significantly lower than that of the single Duffing oscillator subsystem, so this paper further applies the model of the double coupling Duffing oscillator and the Van der Pol-Duffing oscillator.

### C. DIFFERENTIAL DOUBLE COUPLING DUFFING OSCILLATOR AND VAN DER POL-DUFFING OSCILLATOR DETECTION METHOD

The differential detection system can be composed of two chaotic oscillators and form a smaller ratio to carry out differential, so that the differential detection system has better initial value stability. Compared with a single chaotic oscillator which judges the detection result by observing the phase diagram of the system, the timing chart generated by differential generation of the two oscillators makes the result more intuitive and easier to judge. If the detection system is in a large-scale periodic state, the differential timing chart will show a closed curve graph with relatively regular amplitude. If the detection system is in a chaotic state, the differential timing diagram will show an irregular peak diagram with large amplitude swing, which is a chaotic signal. The differential double Duffing oscillator detection model is an improvement based on the single Duffing oscillator model, and the detection result can be judged according to the timing chart generated after difference.

Differential double coupling Duffing oscillator and Van der Pol-Duffing oscillator detection method, named the proposed method 1, is proposed, which forms a smaller ratio for difference. Compared with the differential double Duffing oscillator model, the coupling Duffing oscillator and Van der Pol-Duffing oscillator model replace the single Duffing oscillator, which has better initial value stability. The system

judges through the output timing diagram, making the result more intuitive and easier to judge. In this paper, the model formula of Differential double coupling Duffing oscillator and Van der Pol-Duffing oscillator is proposed as follows:

$$\begin{cases} x_1'' + kx_1' + ax_1^3 - bx_1 + d(x_1 - y_1) = \gamma \cos \omega t \\ y_1'' + \beta(1 + y_1^2)y_1' + y_1 + d(y_1 - x_1) = \gamma \cos \omega t \\ x_2'' + kx_2' + ax_2^3 - bx_2 + d(x_2 - y_2) = \alpha \cdot \gamma \cos \omega t \\ y_2'' + \beta(1 + y_2^2)y_2' + y_2 + d(y_2 - x_2) = \alpha \cdot \gamma \cos \omega t \end{cases} \tag{17}$$

In Equation (17), $\alpha$ is the policy force coefficient that affects different oscillators, and other parameters of the two pairs of coupling Duffing oscillators and Van der Pol-Duffing oscillators are exactly the same except for the different policy forces. The same input signal to be tested is added to the differential coupling Duffing oscillator and Van der Pol-Duffing oscillator detection system, and the weak signal detection model formula is:

The differential display of the two pairs of oscillators is realized by generating $x_1 - x_2$ timing diagram. The $x_1 - x_2$ timing diagram is a regular timing diagram with only amplitude change. When the coefficient $\alpha$ changes, it will not affect the waveform of the differential timing diagram, but only its size. When the amplitude of the poling force of the two pairs of coupled oscillators is the same, that is, $\alpha = 1$, there is no phase difference. When the magnitude of the driving force of the two pairs of coupled oscillators is different, that is, $\alpha \neq 1$, there is a phase difference and the magnitude of the phase difference varies with the change of the coefficient $\alpha$. The coefficient $\alpha$ in this paper is 1.001.

Here, let $n(t)$ be Gaussian white noise with variance $\delta^2 = 0.01$, $\omega = \omega_1 = 1$, $a = b = 1$, $d = 0.2$, $k = 0.5$, sampling frequency is 100Hz, $\gamma = 0.7885$, the amplitude of the analog signal is changed to 0.005, and the differential timing diagram obtained by the differential double Duffing oscillator. The proposed method 1 in each stage are shown in Figure 5 and Figure 6.

As can be seen from Figure 5 and Figure 6, the differential timing diagram generated by the differential system is more convenient to judge the current chaotic system state than the phase diagram generated by the single vibration subsystem and the double coupling vibration subsystem, and the analog signal can be successfully detected with clear and intuitive result.

It can be seen from the above experiments that the proposed method 1 reduces the threshold of detection signal-to-noise ratio by coupling method, and it simplifies the phase diagram judgment process by difference method. In the following, the differential double coupled vibrator detection system is further improved.

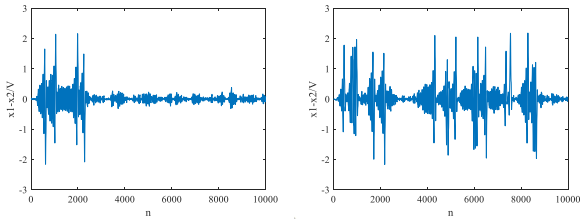


(a) Critical chaotic differential timing diagram (b) Chaotic state when $n(t)$

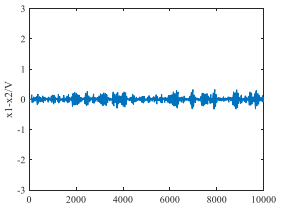


(c) Large scale periodic state when $0.005\cos(t)+n(t)$

**FIGURE 5.** Detection result of differential double Duffing oscillator.

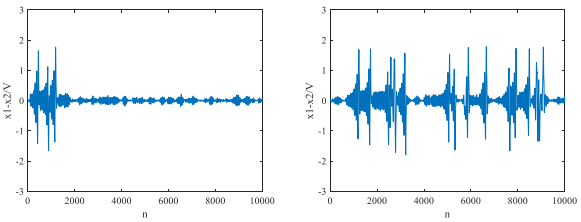


(a) Critical chaotic difference timing diagram (b) Chaotic state when $n(t)$

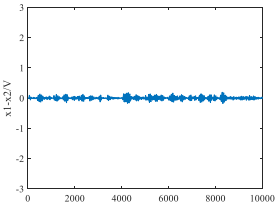


(c) Large scale periodic state when $0.005\cos(t)+n(t)$

**FIGURE 6.** Detection result of the proposed method 1.

## III. DIFFERENTIAL DOUBLE COUPLING DUFFING OSCILLATOR AND VAN DER POL-DUFFING OSCILLATOR VARIABLE STEP-SIZE DETECTION METHOD

### A. PRINCIPLE OF INTERMITTENT CHAOTIC CORRELATION DETECTION

The detection system of differential double coupling Duffing oscillator and Van der Pol-Duffing oscillator is not very effective for weak signal with unknown frequency. In this paper, the variable step-size intermittent chaotic system of differential double coupling Duffing oscillator and Van der Pol-Duffing oscillator is used to detect weak signal with unknown

$$\begin{cases} x'' + kx' + ax^3 - bx + d(x - y) = \gamma \cos \omega t + A \cos \omega_1 t + n(t) \\ y'' + \beta(1 + y^2)y' + y + d(y - x) = \gamma \cos \omega t + A \cos \omega_1 t + n(t) \end{cases} \tag{16}$$

frequency. Intermittent chaos refers to the regular alternation of chaotic state and periodic state. It uses the sensitivity of chaotic oscillator to small disturbance and immunity to noise to detect weak signal [47].

Using the phase change of chaotic oscillator to detect weak periodic signal requires a small frequency difference between the signal to be detected and the policy force built in the system. This frequency difference can cause the detection system to generate chaos and intermittent chaos phenomenon with alternating period. Intermittent chaos is the detection of noisy periodic signal with unknown frequency by using the immunity of chaotic oscillator to noise and the sensitivity of small disturbance. If $s(t)$ is added to the single Duffing oscillator detection system as the signal to be detected, the state equation is:

$$\begin{cases} x' = \omega y \\ y' = \omega(-0.5y + x - x^3 + \gamma_d \cos(\omega t) + s(t)) \end{cases} \tag{19}$$

In Equation (19), the signals to be tested $s(t) = A\cos(\omega' t + \phi)$, $\phi$ are the initial phase of the signal to be tested, $\gamma_d$ is the critical chaos threshold of the system, $\omega' = \omega + \Delta\omega$, $\Delta\omega$ is the frequency difference between the built-in policy power of the system and the signal to be tested. The total policy power $S(t)$ of the system is:

$$S(t) = \gamma_d \cos(\omega t) + A\cos(\omega' t + \phi) = R(t)\cos(\omega t + \theta(t)) \tag{20}$$

In Equation (20), the poling force amplitude $R(t) = \sqrt{\gamma_d^2 + 2\gamma_d A\cos(\Delta\omega t + \phi) + A^2}, A \ll \gamma_d$, the frequency difference between the signal to be measured and the poling force built in the system is $\Delta\omega$, which indicates that the poling force amplitude varies periodically. When the poling force amplitude $R(t) \geq \gamma_d$, the system is in a large-scale periodic state. When the poling force amplitude $R(t) < \gamma_d$, the system is in a chaotic state.

In this paper, the fourth-order Runge-Kutta method is used to carry out numerical algorithm analysis on Duffing oscillator subsystem. Through numerical simulation, the intermittent chaotic frequency difference range of chaotic oscillator is calculated to be $|\Delta\omega/\omega| \leq 0.03$, and the system is in intermittent chaotic state. The frequency difference range of intermittent chaos of double Duffing oscillators is $|\Delta\omega/\omega| < 0.08$, and the system is in intermittent chaos state. The intermittent chaotic frequency difference range $|\Delta\omega/\omega| \leq 0.08$ between the double coupling Duffing oscillator and the Van der Pol-Duffing oscillator, and the system is in an intermittent chaotic state. The frequency difference range of intermittent chaos between the differential double coupling Duffing oscillator and the Van der Pol-Duffing oscillator is $|\Delta\omega/\omega| < 0.09$, and the system is in an intermittent chaotic state. By comparing the frequency difference range of the above four kinds of intermittent chaos, it can be found that the intermittent chaos of differential double coupling Duffing oscillator and Van der Pol-Duffing oscillator can better increase the detection step size, which is convenient to realize the detection of unknown weak signal. Adjusting the proportion and reducing the number of solving steps can reduce the calculation amount of the detection method. The timing chart of intermittent chaos of the double coupling Duffing oscillator and the Van der Pol-Duffing oscillator and the differential double coupling Duffing oscillator and the Van der Pol-Duffing oscillator are shown in Figure 7.

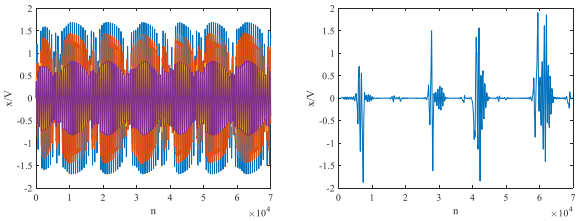

(a) Double coupling Duffing oscillator and Van der Pol-Duffing oscillator

(b) Differential double coupling Duffing oscillator and Van der Pol-Duffing oscillator

**FIGURE 7.** The timing diagram of two intermittent chaotic methods.

### B. DIFFERENTIAL DOUBLE COUPLING DUFFING OSCILLATOR AND VAN DER POL-DUFFING OSCILLATOR VARIABLE STEP-SIZE DETECTION METHOD

The variable step-size intermittent chaos detection method is to change the solution step-size of the solution process of the differential double coupling Duffing oscillator and the Van der Pol-Duffing oscillator, convert the signal to be detected and the policy term of the built-in policy force into corresponding discrete sequences, and judge whether the signal is successfully detected by observing the output timing chart $x_1 - x_2$ at this time. The built-in policy force sequence interval of the detection model is the solution step-size of the system, and the sequence interval of the signal to be detected is $T_s(T_s = 1/f_s, f_s$ is the sampling frequency of the signal to be detected). The detection result has nothing to do with the solution step size but only with the sampling frequency, so the system can be adjusted to an intermittent chaotic state by changing the solution step size of the detection system to complete the signal detection.

When the differential double coupling Duffing oscillator and Van der Pol-Duffing oscillator are used for variable

$$\begin{cases} x_1'' + kx_1' + ax_1^3 - bx_1 + d(x_1 - y_1) = \gamma\cos\omega t + A\cos\omega_1 t + n(t) \\ y_1'' + \beta(1 + y_1^2)y_1' + y_1 + d(y_1 - x_1) = \gamma\cos\omega t + A\cos\omega_1 t + n(t) \\ x_2'' + kx_2' + ax_2^3 - bx_2 + d(x_2 - y_2) = \alpha\cdot\gamma\cos\omega t + A\cos\omega_1 t + n(t) \\ y_2'' + \beta(1 + y_2^2)y_2' + y_2 + d(y_2 - x_2) = \alpha\cdot\gamma\cos\omega t + A\cos\omega_1 t + n(t) \end{cases} \tag{18}$$

step-size intermittent chaos detection, the total policy term in Equation (18) is $\gamma \cos \omega t + A \cos \omega_1 t$ and $\alpha \cdot \gamma \cos \omega t + A \cos \omega_1 t$, the system is in an intermittent chaotic state, and the solution step-size of the system is $h = \frac{\omega'}{l\omega f_s}$, $\omega' = \omega + \Delta\omega, l \in (0.94, 1.06)$. The policy term of the two chaotic oscillators is discretized into:

$$\begin{cases} S_{n1} = 0.7885 \cdot \cos\left(\dfrac{n\omega'}{lf_s}\right) + A\cos\left(\dfrac{n\omega'}{f_s}\right) \\ S_{n2} = 1.001 \cdot 0.7885\cos\left(\dfrac{n\omega'}{lf_s}\right) + A\cos\left(\dfrac{n\omega'}{f_s}\right) \end{cases} \tag{21}$$

If $n = 1, 2, \ldots, N$, the frequency difference between the built-in driving force and the sinusoidal signal conforms to the frequency difference of intermittent chaos, so the system will have intermittent chaos. In this paper, differential double coupling Duffing oscillator and Van der Pol-Duffing oscillator variable step-size detection method is proposed. Its step flow chart is shown in Figure 8. The specific steps are as follows:

(1) Adjust the parameters of two coupling Duffing oscillator and Van der Pol-Duffing oscillator, $\gamma = 0.7885, \omega_1 = 1 rad/s, \alpha = 1.001, d = 0.2$.

(2) Input the signal $A\cos(\omega_1 t) + n(t)$ into the signal detection system, make the frequency be 1kHz, and use step $a_n = \frac{1.06^n \times 2\pi}{1.06 \times \omega \times f_s}$ to solve it, where $n = 1, 2, \ldots, N$.

(3) Adjust the solution step size and observe the differential timing diagram $x_1 - x_2$ output by the differential double coupling detection system. If the system exhibits intermittent chaos under the two adjacent solution step lengths $a_n$ and $a_{n+1}$, the existence of sinusoidal signals is detected. Otherwise, return to (2).

(4) $\omega_n$ and $\omega_{n+1}$ corresponding to two adjacent solving steps $a_n$ and $a_{n+1}$ are calculated through $\omega_n = 1.06^n rad/s$. Then the sine signal angular frequency is $\omega'' = \frac{\omega_n + \omega_{n+1}}{2} rad/s$.

The variable step intermittent chaos of the three detection systems is detected by taking $a_n = \frac{1.06^n \times 2\pi}{1.06 \times \omega \times f_s}$ as the solution step of the detection system, including double coupling Duffing oscillator and Van der Pol-Duffing oscillator subsystem, differential double Duffing oscillator subsystem, differential double coupling Duffing oscillator and Van der Pol-Duffing oscillator subsystem. Input the signal $S_{n1} = A\cos(10t) + n(t)$ into the system, where $n(t)$ is Gaussian white noise with variance $\delta^2 = 0.01$, $A$ is adjusted, $d = 0.2$, angular frequency $\omega = 1 rad/s$, $\gamma = 0.7885$. The output timing diagrams of three detection methods are shown in Figure 9.

The three systems will show intermittent chaotic state when the solution step is $a_{39}$, and the signal can be detected at this time. It can be seen from (c) and (e) in Figure 9 that the timing diagrams of differential double Duffing oscillator and the proposed method 2 are relatively easy to distinguish detection signal. The double coupling Duffing oscillator and the Van der Pol-Duffing oscillator subsystem, the differential double Duffing oscillator subsystem, and the differential double coupling Duffing oscillator and the Van der Pol-Duffing oscillator subsystem can detect the periodic signal amplitude

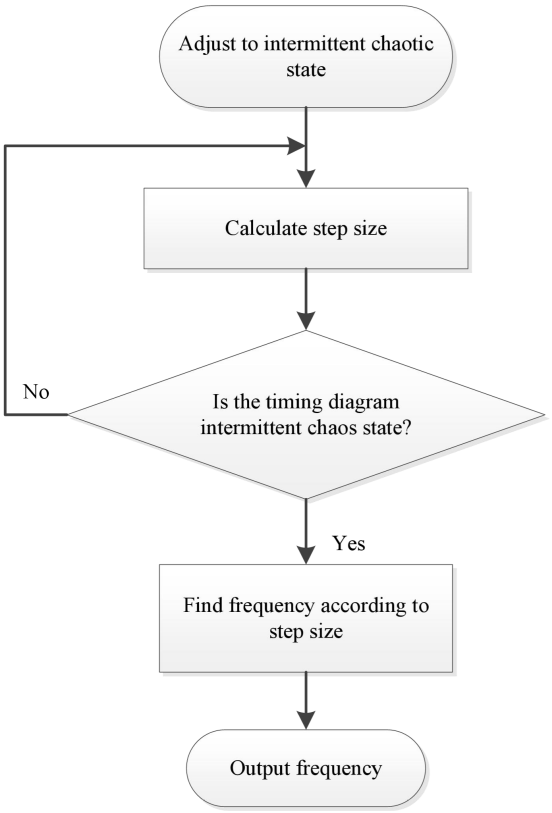


**FIGURE 8.** Step flow chart of the proposed method 2.

$A > 0.020$, $A > 0.014$, and $A > 0.011$ respectively. According to the SNR calculation Equation (13), the lowest SNR of the detection signal of the double coupling Duffing oscillator and the Van der Pol-Duffing oscillator subsystem, the differential double Duffing oscillator, and the proposed method 2 is $-16.99$dB, $-20.73$dB, and $-23.01$dB respectively. Its SNR threshold is respectively reduced by 6.02dB and 2.28dB.

Due to different intermittent chaotic frequency differences, each system can form a new detection step-size and bandwidth by changing the common ratio. Through the different scale ranges of different methods, the number of solving steps can better reduce the calculation amount. The detection methods such as Duffing oscillator, double Duffing oscillator, differential double Duffing oscillator, double coupling Duffing oscillator and Van der Pol-Duffing oscillator and the proposed method 2 are compared in Table 1. Table 1 shows that the number of solving steps of the proposed method 2 is obviously smaller than that of other methods, and the required calculation amount is also smaller than that of other methods.

### C. ANALOG SIGNAL DETECTION UNDER DIFFERENT DISTRIBUTED NOISE BACKGROUND

Gaussian white noise, Gaussian color noise [48], Rayleigh distribution noise [49] and $K$ distribution noise [50] can all well simulate underwater acoustic environment noise. In order to verify the detection capability of the proposed method 2, Gaussian white noise, Gaussian color noise and

**TABLE 1.** Data of each detection system.

| Method | Parameter | | |
|---|---|---|---|
| | Common Ratio | Number of Solving Steps | Detection Bandwidth |
| Duffing oscillator | 1.01<br>1.02<br>1.03 | 232<br>117<br>78 | $(0.99,1.01)\cdot\omega$<br>$(0.98,1.02)\cdot\omega$<br>$(0.97,1.03)\cdot\omega$ |
| Double Duffing oscillator | 1.05<br>1.06<br>1.07 | 48<br>40<br>35 | $(0.95,1.05)\cdot\omega$<br>$(0.94,1.06)\cdot\omega$<br>$(0.93,1.07)\cdot\omega$ |
| Differential double Duffing oscillator | 1.05<br>1.06<br>1.07 | 48<br>40<br>35 | $(0.95,1.05)\cdot\omega$<br>$(0.94,1.06)\cdot\omega$<br>$(0.93,1.07)\cdot\omega$ |
| Double coupling Duffing oscillator and Van der Pol-Duffing oscillator | 1.06<br>1.07<br>1.08 | 40<br>35<br>30 | $(0.94,1.06)\cdot\omega$<br>$(0.93,1.07)\cdot\omega$<br>$(0.92,1.08)\cdot\omega$ |
| The proposed method 2 | 1.07<br>1.08<br>1.09 | 35<br>30<br>26 | $(0.93,1.07)\cdot\omega$<br>$(0.92,1.08)\cdot\omega$<br>$(0.91,1.09)\cdot\omega$ |

Rayleigh distribution noise are used as analog signal noise background.

#### 1) ANALOG SIGNAL DETECTION UNDER GAUSSIAN WHITE NOISE

In general, the underwater acoustic signal noise in a short period of time follows Gaussian distribution [51], [52]. It is generated by many sound sources with random phase and random amplitude. The instantaneous value of Gaussian white noise obeys Gaussian distribution and the power spectral density distribution is uniform. It is an ideal model to simulate the background noise of underwater acoustic signal. The timing diagram and probability distribution diagram of Gaussian white noise are shown in Figure 10.

In actual weak signal detection, there will be multiple signals to be detected under the same strong noise background. Here, the signal $S_{n1} = A\cos(10t) + n(t)$ is changed to the signal $S_{n1} = 0.01\cos(10t) + 0.01\cos(30t) + n(t)$, where $n(t)$ is Gaussian white noise with variance $\delta^2 = 0.01$, sampling frequency is 1kHz. The power spectral density diagram of $S_{n1}$ is shown in Figure 11.

The detection result of the proposed method 2 is shown in Figure 12.

In Figure 12, the system shows intermittent chaos when detecting adjacent step size, and detects two signals with different frequencies. When the adjacent step size are $a_{39}$ and $a_{40}$, the corresponding sizes of $f_{39}$ and $f_{40}$ are 9.704Hz and 10.286Hz, then the system's determination frequency at this time is $f_1' = 9.995$Hz. When the adjacent steps are $a_{58}$ and $a_{59}$ and the corresponding sizes of $f_{58}$ and $f_{59}$ are 29.359Hz and 31.120Hz, the system's decision frequency is $f_2' = 30.239$Hz at this time. When the frequency of the signal to be tested is 10Hz and 30Hz respectively, the average error rate can be calculated to be 0.423%, that is, the system can better detect the multi-frequency signal under the same strong Gaussian white noise background and accurately obtain the frequency of the signal to be tested.

#### 2) ANALOG SIGNAL DETECTION UNDER GAUSSIAN COLOR NOISE

The marine environmental noise is composed of a large number of noise sources. According to the central limit theorem of statistics, under very wide conditions, the distribution of the sum of N statistically independent random variables tends to Gaussian distribution under the limit of $N \to \infty$. So its amplitude distribution should be Gaussian. Strictly speaking,

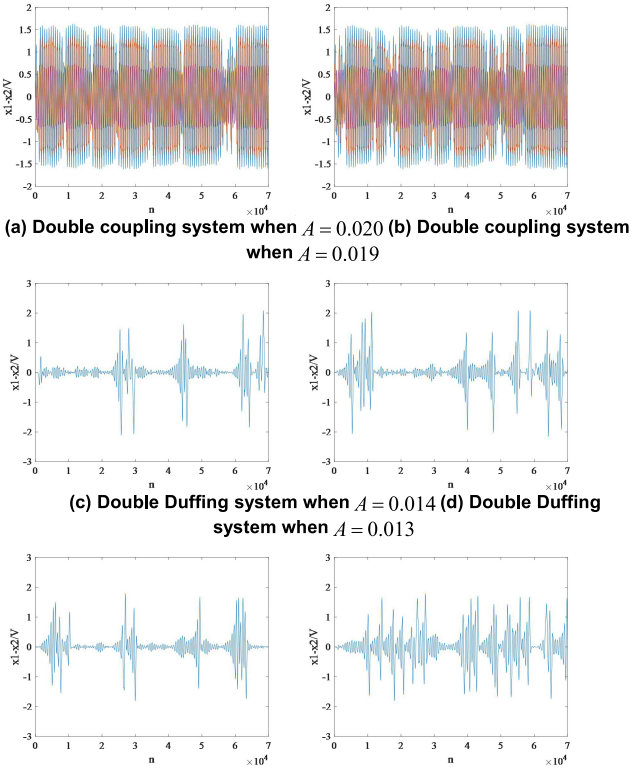


(a) Double coupling system when $A = 0.020$ (b) Double coupling system when $A = 0.019$

(c) Double Duffing system when $A = 0.014$ (d) Double Duffing system when $A = 0.013$

(e) The proposed method 2 when $A = 0.011$ (f) The proposed method 2 when $A = 0.010$

**FIGURE 9.** Output timing diagram of three detection methods.

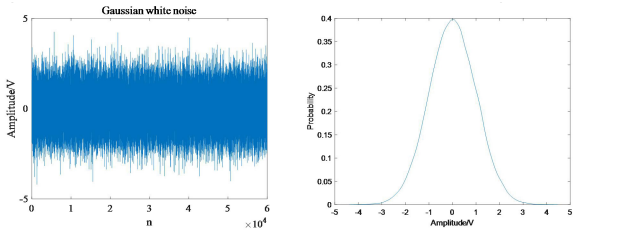


(a) Timing diagram (b) Probability distribution diagram

**FIGURE 10.** Timing diagram and probability distribution diagram of Gaussian white noise.

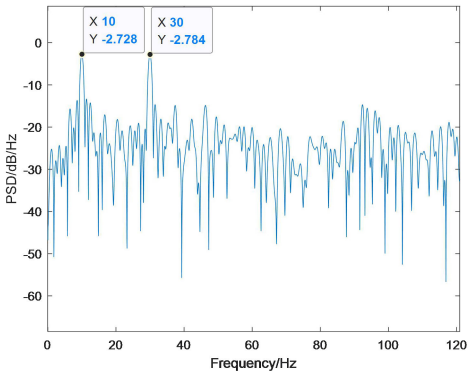


**FIGURE 11.** Power spectral density diagram of $S_{n1}$.

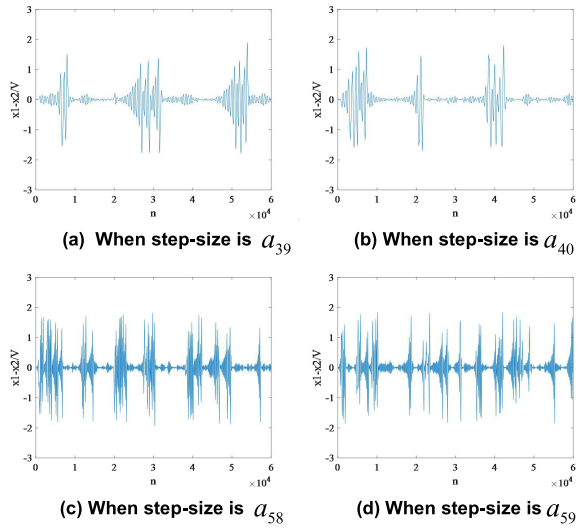


(a) When step-size is $a_{39}$ (b) When step-size is $a_{40}$

(c) When step-size is $a_{58}$ (d) When step-size is $a_{59}$

**FIGURE 12.** The detection result of the proposed method 2 for signal $S_{n1}$.

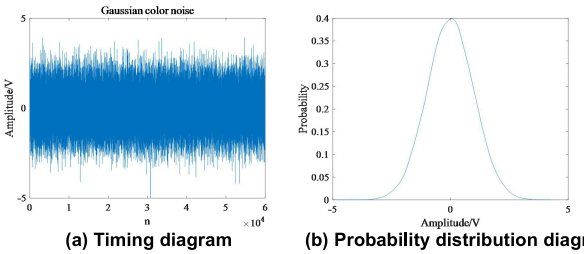


(a) Timing diagram (b) Probability distribution diagram

**FIGURE 13.** Timing diagram and probability distribution diagram of Gaussian color noise.

the marine environmental noise is anisotropic. In the simulation process, the marine environmental noise is simplified and approximately regarded as color noise obeying Gaussian distribution [53]. The timing diagram and probability distribution diagram of Gaussian color noise are shown in Figure 13.

$S_{n2} = 0.01\cos(20t) + 0.01\cos(40t) + n(t)$ is the signal to be measured, and $n(t)$ is Gaussian color noise with variance 0.01, sampling frequency is 1kHz. The power spectral density diagram of $S_{n2}$ is shown in Figure 14.

The detection result of the proposed method 2 is shown in Figure 15.

In Figure 15, when the adjacent step-sizes are $a_{51}$ and $a_{52}$ and the corresponding sizes of $f_{51}$ and $f_{52}$ are 19.525Hz and 20.697Hz, the system's decision frequency at this time is $f_3' = 20.111$Hz. When the adjacent steps are $a_{63}$ and $a_{64}$ and the corresponding sizes of $f_{63}$ and $f_{64}$ are 39.289Hz and 41.646Hz, the system's decision frequency at this time is $f_4' = 40.467$Hz. When the frequency of the signal to be tested is 20Hz and 40Hz respectively, the average error rate can be calculated to be 0.855%. So the system can better detect the multi-frequency signal to be tested under the same strong Gaussian color noise background and accurately obtain the frequency of the signal to be tested.

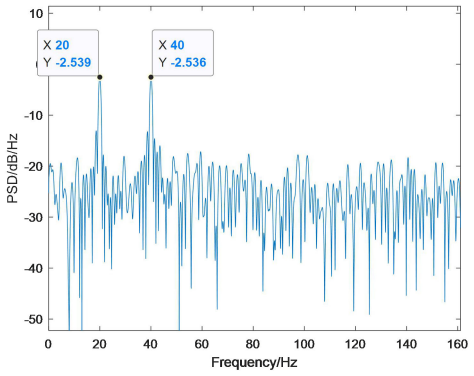


**FIGURE 14.** Power spectral density diagram of $S_{n2}$.

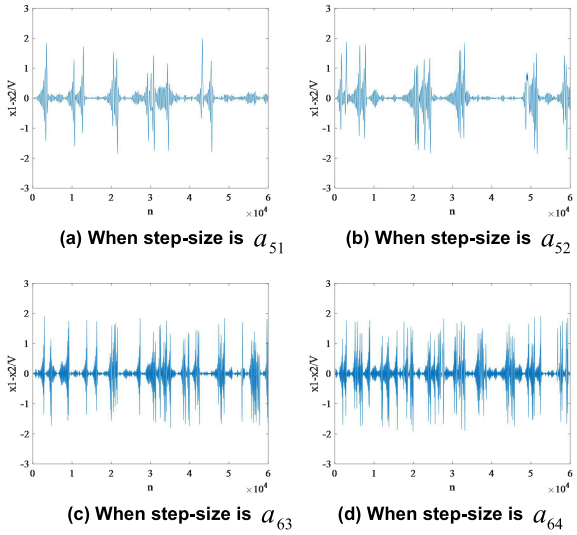


(a) When step-size is $a_{51}$ (b) When step-size is $a_{52}$

(c) When step-size is $a_{63}$ (d) When step-size is $a_{64}$

**FIGURE 15.** The detection result of the proposed method 2 for signal $S_{n2}$.

### 3) ANALOG SIGNAL DETECTION UNDER RAYLEIGH DISTRIBUTION NOISE

Rayleigh distribution is the most common type of distribution that describes the statistical time-varying characteristics of flat fading signal reception envelope or independent multi-path component reception envelope. The envelope of the sum of two orthogonal Gaussian noise signals follows Rayleigh distribution. Therefore, the noise obeying Rayleigh distribution can well simulate the noise in underwater acoustic signal [49]. The timing diagram and probability distribution diagram of Rayleigh distribution noise are shown in Figure 16.

The signal to be measured is $S_{n3} = 0.01\cos(50t) + 0.01\cos(60t) + n(t)$, and $n(t)$ is Rayleigh distribution noise with variance 0.01, sampling frequency is 1kHz. The power spectral density diagram of $S_{n3}$ is shown in Figure 17.

The detection result of the proposed method 2 is shown in Figure 18.

In Figure 18, when the adjacent step-sizes are $a_{67}$ and $a_{68}$ and the corresponding sizes of $f_{67}$ and $f_{68}$ are 49.601Hz

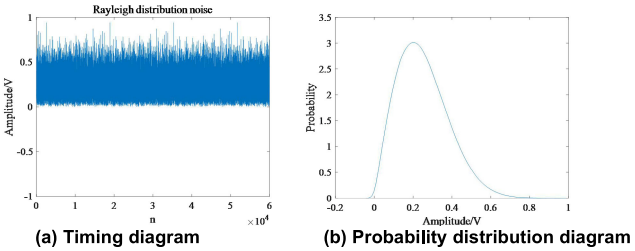


(a) Timing diagram (b) Probability distribution diagram

**FIGURE 16.** Timing diagram and probability distribution diagram of Rayleigh distribution noise.

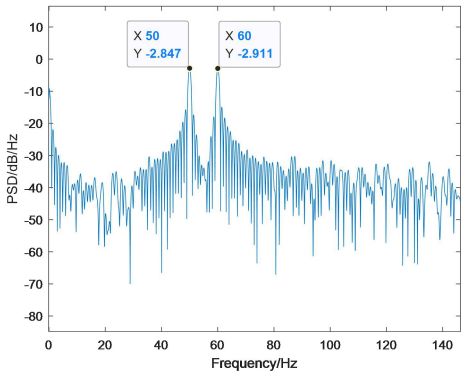


**FIGURE 17.** Power spectral density diagram of $S_{n3}$.

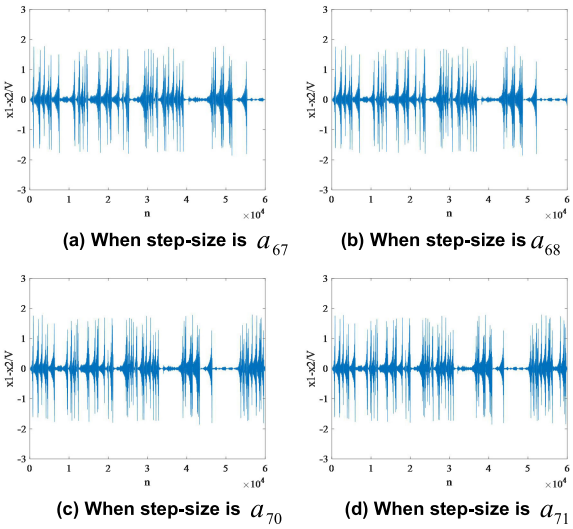


(a) When step-size is $a_{67}$ (b) When step-size is $a_{68}$

(c) When step-size is $a_{70}$ (d) When step-size is $a_{71}$

**FIGURE 18.** The detection result of the proposed method 2 for signal $S_{n3}$.

and 52.577Hz, the system's decision frequency at this time is $f_5' = 51.088$Hz. When the adjacent steps are $a_{70}$ and $a_{71}$, the corresponding sizes of $f_{70}$ and $f_{71}$ are 59.076Hz and 62.620Hz, then the system's decision frequency at this time is $f_6' = 60.848$Hz. When the frequency of the signal to be tested is 50Hz and 60Hz respectively, the average error rate can be calculated to be 3.265%. So the system can better detect the multi-frequency signal to be tested under the same strong Rayleigh distribution noise background and accurately obtain the frequency of the signal to be tested.

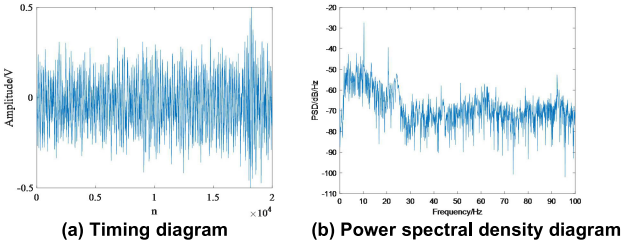


(a) Timing diagram (b) Power spectral density diagram

**FIGURE 19.** Timing diagram and power spectral density diagram of the measured signals.

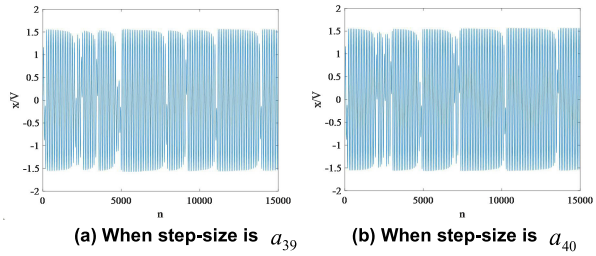


(a) When step-size is $a_{39}$ (b) When step-size is $a_{40}$

**FIGURE 20.** Detection results of double coupling Duffing oscillator and Van der Pol-Duffing oscillator variable step-size detection method.

## IV. DETECTION OF MEASURED SHIP-RADIATED NOISE SIGNAL

In this paper, the measured marine environment background noise signal obtained from the ship noise database website http://atlanttic.uvigo.es/underwaternoise/ is used to verify the effectiveness of the proposed method, whose sampling frequency is 52734Hz [54]. In order to facilitate detection, sample the measured data again, sampling frequency is 1kHz, the underwater acoustic signal data are intercepted and normalized to be input into the detection system. The power spectral density diagram can roughly give the frequency range. We compare the peak frequency with the signal frequency detected by the proposed method 2 in order to verify its effectiveness. The timing diagram and power spectral density diagram of the measured signals are shown in Figure 19.

By observing the power spectral density diagram in Figure 19, it can be roughly determined that the signal frequency floats at about 10Hz. In order to detect the actually measured signal, the step-size is set to $a_n = \frac{1.06^n \times 2\pi}{1.06 \times 1 \times f_s}$. Based on variable step-size intermittent chaos theory, the adjacent intermittent chaotic timing diagram output by double coupling Duffing oscillator and Van der Pol-Duffing oscillator method, differential double Duffing oscillator method proposed in 2020 [26] and the proposed method 2 are shown in Figure 20, Figure 21 and Figure 22.

At this time, the adjacent step-sizes are $a_{39}$ and $a_{40}$, and the displayed timing chart is intermittent chaotic state, which indicates that the signal can be detected. The corresponding frequencies are $f_{39} = 9.7035$Hz and $f_{40} = 10.2857$Hz respectively, and the spectrum frequency of underwater acoustic signal is $f' = \frac{f_{39}+f_{40}}{2} \approx 9.9946$Hz.

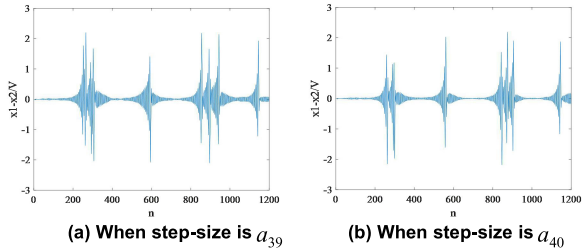


(a) When step-size is $a_{39}$ (b) When step-size is $a_{40}$

**FIGURE 21.** Detection results of differential double Duffing oscillator variable step-size detection method proposed in 2020 [26].

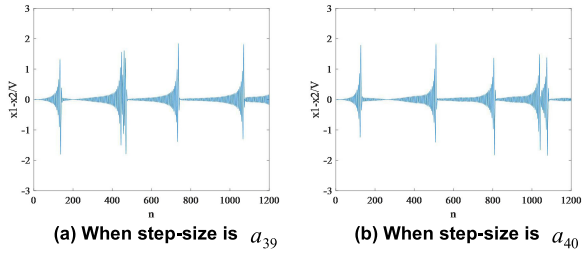


(a) When step-size is $a_{39}$ (b) When step-size is $a_{40}$

**FIGURE 22.** Detection results of the proposed method 2.

By comparing Figure 20, Figure 21 and Figure 22, it can be found that the detection result diagram of the proposed method 2 is clearer and more intuitive and has higher identification degree than that of the other two methods.

## V. DISCUSSIONS

There are some problems in the results of traditional chaotic detection methods, such as not intuitive enough detection result, large judgment error, and not ideal detection effect of signals with low SNR. This paper combines the theory of difference and coupling between chaotic oscillators. A detection method of differential double coupling Duffing oscillator and Van der Pol-Duffing oscillator is proposed to improve the problems existing in traditional detection methods. In view of its excellent detection performance, it will have broad research value in other weak signal applications, such as mechanical fault diagnosis, spectral research, acoustic telemetry, and so on.

In view of the problems of parameter estimation and detection performance of traditional detection methods in the field of unknown frequency signal, a differential double coupling Duffing oscillator and Van der Pol-Duffing oscillator variable step-size detection method based on intermittent chaos theory is proposed to improve the detection performance. Experiments show that it can detect the analog signals in three different noise backgrounds. It also has a good effect on the detection of measured underwater acoustic signals. In the future, it can be applied to detect general periodic signal with unknown frequency.

## VI. CONCLUSION

A new detecting method for underwater acoustic weak signal based on differential double coupling oscillator is proposed. The main conclusions of this article are as follows:

(1) For weak signal detection with known frequency, based on the double coupling Duffing oscillator method, a differential double coupling Duffing oscillator and Van der Pol-Duffing oscillator detection method is proposed. Its feasibility is verified by sinusoidal analog signal. It has intuitive detection effect and high sensitivity, and can detect weak signal with lower SNR.

(2) For underwater acoustic weak signal detection with unknown frequency, a differential double coupling Duffing oscillator and Van der Pol-Duffing oscillator variable step-size detection method is proposed. It can increase detection bandwidth, reduce calculation amount and complexity. Its SNR is 2.28dB lower than that of the differential double Duffing oscillator variable step-size detection method. Its feasibility is verified by sinusoidal analog signal under Gaussian white noise, Gaussian color noise and Rayleigh distribution noise. Its detection effect is verified in the detection of measured underwater acoustic signals. It provides a new detecting method for underwater acoustic weak signal. In the future, it can be applied to detect weak periodic signal such as square wave and general periodic signal with unknown frequency.

## REFERENCES

[1] N. Y. Muzychenko, "Search and detection of noise-like signals under communication channel frequency-instability conditions," *J. Commun. Technol. Electron.*, vol. 64, no. 3, pp. 245–250, 2019.

[2] W. Li, S. Zhou, P. Willett, and Q. Zhang, "Preamble detection for underwater acoustic communications based on sparse channel identification," *IEEE J. Ocean. Eng.*, vol. 44, no. 1, pp. 256–268, Jan. 2019.

[3] S. Siddagangaiah, Y. Li, X. Guo, X. Chen, Q. Zhang, K. Yang, and Y. Yang, "A complexity-based approach for the detection of weak signals in ocean ambient noise," *Entropy*, vol. 18, no. 3, Mar. 2016, Art. no. 101.

[4] Z.-H. Lai and Y.-G. Leng, "Weak-signal detection based on the stochastic resonance of bistable duffing oscillator and its application in incipient fault diagnosis," *Mech. Syst. Signal Process.*, vol. 81, pp. 60–74, Dec. 2016.

[5] Z. Li, H. Su, S. Zhou, and Q. Hu, "Signal fusion-based targets detection in the presence of clutter and subspace interference for multiple-input-multiple-output radar," *IET Radar, Sonar Navigat.*, vol. 13, no. 1, pp. 148–155, Jan. 2019.

[6] D.-P. Xia, Y. Zhang, P. Cai, and L. Huang, "An energy-efficient signal detection scheme for a radar-communication system based on the generalized approximate message-passing algorithm and low-precision quantization," *IEEE Access*, vol. 7, pp. 29065–29075, 2019.

[7] H. Dong, K. He, X. Shen, S. Ma, H. Wang, and C. Qiao, "Adaptive intrawell matched stochastic resonance with a potential constraint aided line enhancer for passive sonars," *Sensors*, vol. 20, no. 11, p. 3269, Jun. 2020.

[8] Y. Zheng, X. Chen, and R. Zhu, "Frequency hopping signal detection based on wavelet decomposition and Hilbert–Huang transform," *Modern Phys. Lett. B*, vol. 31, nos. 19–21, Jul. 2017, Art. no. 1740078.

[9] E. Pomponi, A. Vinogradov, and A. Danyuk, "Wavelet based approach to signal activity detection and phase picking: Application to acoustic emission," *Signal Process.*, vol. 115, pp. 110–119, Oct. 2015.

[10] M. J. Hinich, "Detecting a transient signal by bispectral analysis," *IEEE Trans. Acoust., Speech, Signal Process.*, vol. 38, no. 7, pp. 1277–1283, Jul. 1990.

[11] S. Colonnese and G. Scarano, "Transient signal detection using higher order moments," *IEEE Trans. Signal Process.*, vol. 47, no. 2, pp. 515–520, Feb. 1999.

[12] V. Chandran, S. Elgar, and A. Nguyen, "Detection of mines in acoustic images using higher order spectral features," *IEEE J. Ocean. Eng.*, vol. 27, no. 3, pp. 610–618, Jul. 2002.

[13] M.-J. Sheu, P.-Y. Lin, J.-Y. Chen, C.-C. Lee, and B.-S. Lin, "Higher-order-statistics-based fractal dimension for noisy bowel sound detection," *IEEE Signal Process. Lett.*, vol. 22, no. 7, pp. 789–793, Jul. 2015.

[14] E. Palahina, M. Gamcová, I. Gladišová, J. Gamec, and V. Palahin, "Signal detection in correlated non-Gaussian noise using higher-order statistics," *Circuits, Syst., Signal Process.*, vol. 37, no. 4, pp. 1704–1723, Apr. 2018.

[15] W. Miller, T. McKenna, and C. Lau, "Office of naval research contributions to neural networks and signal processing in oceanic engineering," *IEEE J. Ocean. Eng.*, vol. 17, no. 4, pp. 299–307, Oct. 1992.

[16] W. Shao, J. Barras, and P. Kosmas, "Detection of extremely weak NQR signals using stochastic resonance and neural network theories," *Signal Process.*, vol. 142, pp. 96–103, Jan. 2018.

[17] L. Y. Su, L. Deng, W. L. Zhu, and S. L. Zhao, "Statistical detection of weak pulse signal under chaotic noise based on Elman neural network," *Wireless Commun. Mobile Comput.*, vol. 2020, Jan. 2020, Art. no. 9653586.

[18] Z. Qiao, Y. Lei, and N. Li, "Applications of stochastic resonance to machinery fault detection: A review and tutorial," *Mech. Syst. Signal Process.*, vol. 122, pp. 502–536, May 2019.

[19] N. Li, X. K. Li, and C. H. Liu, "Detection method of a short-time Duffing oscillator array with variable amplitude coefficients," *J. Harbin Eng. Univ.*, vol. 37, no. 12, pp. 1645–1652, 2016.

[20] S. Zhou and C. S. Lin, "Application of chaos theory for weak signal of ship detecting," *J. Wuhan Univ. Technol.*, vol. 33, no. 1, pp. 161–164, 2009.

[21] S. Q. Li and X. Z. Wu, "Application of ALE based on FTF algorithm in ship-radiated noise detection," *Commun. Technol.*, vol. 50, no. 6, pp. 1175–1180, 2017.

[22] Q. W. Sun and J. F. Zhang, "Weak signal detection based on improved chaotic oscillator system with dual coupling," *Comput. Mod.*, no. 1, pp. 17–21, 2012.

[23] Z. Y. Shi, S. P. Yang, and Z. H. Zhao, "Weak signal detection based on coupled chaotic oscillator," *J. Shijiazhuang Tiedao Univ.*, vol. 32, no. 1, pp. 18–23, 2019.

[24] K. Wang, X. P. Yan, Q. Yang, X. H. Hao, and J. T. Wang, "Weak signal detection based on strongly coupled Duffing-Van der Pol oscillator and long short-term memory," *J. Phys. Soc. Jpn.*, vol. 89, no. 1, 2020, Art. no. 014003.

[25] Y. F. Wu, S. P. Huang, and G. B. Jin, "Study on partial discharge signal detection by coupled Duffing oscillators," *Acta Phys. Sinica*, vol. 62, no. 13, 2013, Art. no. 130505.

[26] G. H. Li, K. Zhao, and H. Yang, "A new method for detecting line spectrum of ship-radiated noise based on a new double duffing oscillator differential system," *Indian J. Geo Mar. Sci.*, vol. 49, no. 1, pp. 34–43, 2020.

[27] Q. B. Wang, Y. J. Yang, and X. Zhang, "Detection of weak signal based on parameter identification of delay differential system with noise disturbance," *Math. Problems Eng.*, vol. 2020, Apr. 2020, Art. no. 2047952.

[28] M. Wang, Y. Yan, and H. F. Zhang, "Frequency detection of weak signal based on double differential duffing oscillators," *J. Circuits Syst.*, vol. 15, no. 2, pp. 118–121, 2010.

[29] H.-H. Peng, X.-M. Xu, B.-C. Yang, and L.-Z. Yin, "Implication of two-coupled differential van der pol duffing oscillator in weak signal detection," *J. Phys. Soc. Jpn.*, vol. 85, no. 4, Apr. 2016, Art. no. 044005.

[30] Y. Y. Hu, F. L. Zeng, and S. G. Zhang, "New method of complex-frequency signal detection based on double oscillator difference system," *Comput. Eng. Appl.*, vol. 50, no. 16, pp. 206–210, and 264, 2014.

[31] C. Li, X. Xu, Y. Ding, L. Yin, and B. Dou, "Weak photoacoustic signal detection based on the differential duffing oscillator," *Int. J. Modern Phys. B*, vol. 32, no. 9, Apr. 2018, Art. no. 1850103.

[32] R. L. Tian, Z. J. Zhao, and Y. Xu, "Variable scale-convex-peak method for weak signal detection," *Sci. China Technol. Sci.*, vol. 63, 2020, doi: 10.1007/s11431-019-1530-4.

[33] C. P. Ji, S. N. Xu, and W. J. Ji, "Improved weak signal detection for inverse phase transition of Duffing oscillator," *J. Data Acquisition Process.*, vol. 34, no. 2, pp. 223–233, 2019.

[34] Y. Li, P. Lu, B. J. Yang, and X. P. Zhao, "Applying a special kind of two coupled Duffing oscillator system to detect periodic signals under the background of strong colored noise," *Acta Phys. Sinica*, vol. 55, no. 4, pp. 1672–1677, 2006.

[35] Y.-F. Ling, C.-X. Chen, D.-Z. Niu, and T. Chen, "Weak signal detection using double-well Duffing–van der pol oscillator and formulation of detection statistics," *J. Phys. Soc. Jpn.*, vol. 88, no. 4, Apr. 2019, Art. no. 044001.

[36] Z. Y. Shi, S. P. Yang, and Z. H. Zhao, "Research on weak signal detection based on coupled Van der Pol-Duffing system," *China Meas. Test*, vol. 44, no. 8, pp. 107–112, and 119, 2018.

[37] B.-F. Cao, P. Li, X.-Q. Li, X.-Q. Zhang, W.-S. Ning, R. Liang, X. Li, M. Hu, and Y. Zheng, "Detection and parameter estimation of weak pulse signal based on strongly coupled duffing oscillators," *Acta Phys. Sinica*, vol. 68, no. 8, 2019, Art. no. 080501.

[38] L. Li, C. G. Liu, S. Shi, and X. D. Zhang, "A method of weak signal detection based on chaotic oscillator and Lyapunov exponent," *J. Natural Sci. Heilongjiang Univ.*, vol. 29, no. 4, pp. 556–560, 2012.
[39] G. Z. Li, N. L. Tan, S. Q. Su, and C. Zhang, "Unknown frequency weak signal detection based on Lorenz chaotic synchronization system," *J. Vib. Shock*, vol. 38, no. 5, pp. 155–161, 2019.
[40] G. Z. Li and B. Zhang, "Novel method for detecting weak signal with unknown frequency based on Duffing oscillator," *Chin. J. Sci. Instrum.*, vol. 38, no. 1, pp. 181–189, 2017.
[41] J. M. Liu, S. H. Feng, L. N. Ren, and F. C. Liu, "Study on using intermittent chaos to detect unknown frequency signal in noise," *Acta Metrol. Sinica*, vol. 40, no. 3, pp. 472–476, 2019.
[42] P. M. Shi, Y. L. Sun, and D. Y. Han, "Study on variable scale weak signal detection method based on two coupled chaotic oscillator," *Acta Metrol. Sinica*, vol. 37, no. 3, pp. 310–313, 2016.
[43] J. P. Wu, Y. F. Qu, and X. Z. Cheng, "Study on weak signal detection method based on Duffing oscillator," *Electron. Meas. Technol.*, vol. 40, no. 3, pp. 143–146, and 162, 2017.
[44] C. Cong, N. Yu, and H. W. Wang, "Detection and estimation of the harmonics in power system based on approximate entropy and chaotic oscillator," *Electr. Meas. Instrum.*, vol. 53, no. 18, pp. 45–50, 2016.
[45] Y. Li, Y. W. Shi, H. T. Ma, and B. J. Yang, "Chaotic detection method for weak square wave signal submerged in colored noise," *Acta Electronica Sinica*, vol. 32, no. 1, pp. 87–90, 2004.
[46] Z. Y. Shi, S. P. Yang, and Z. H. Zhao, "Research on weak signal detection based on Van der Pol-Duffing oscillator and cross correlation," *J. Shijiazhuang Tiedao Univ.*, vol. 32, no. 2, pp. 66–71, 2019.
[47] Z. G. Chen, Y. A. Li, and X. Chen, "Underwater acoustic weak signal detection based on Hilbert transform and intermittent chaos," *Acta Phys. Sinica*, vol. 64, no. 20, 2015, Art. no. 200502.
[48] Y. S. Qi, "Research on weak underwater target signal detection based on chaotic oscillator," M.S. thesis, School Mar. Sci. Technol., Northwestern Polytech. Univ., Xi'an, China, 2007.
[49] N. Li, "Research on Duffing oscillator detection method for underwater weak target signals," Ph.D. dissertation, College Underwater Acoust. Eng., Harbin Eng. Univ., Harbin, China, 2017.
[50] D. A. Abraham and A. P. Lyons, "Novel physical interpretations of K-distributed reverberation," *IEEE J. Ocean. Eng.*, vol. 27, no. 4, pp. 800–813, Oct. 2002.
[51] X. Liu, Y. Zhou, and J. L. Xiang, "High order spectrum for detecting Gaussianity and linearity of ocean ambientand ship noise," *J. Data Acquisition Process.*, vol. 15, no. 3, pp. 301–306, 2000.
[52] J. Aparicio, A. Jimenez, J. Urena, and F. J. Alvarez, "Realistic modeling of underwater ambient noise and its influence on spread-spectrum signals," in *Proc. OCEANS*, Genova, Italy, May 2015, pp. 18–21.
[53] G. L. Zhou, G. H. Li, and J. Cheng, "A new method of underwater acoustic signal detection under the background of marine environmental noise," *Acoust. Electron. Eng.*, no. 2, pp. 21–23 and 27, 2009.
[54] D. Santos-Domínguez, S. Torres-Guijarro, A. Cardenal-López, and A. Pena-Gimenez, "ShipsEar: An underwater vessel noise database," *Appl. Acoust.*, vol. 113, pp. 64–69, Dec. 2016.

**GUOHUI LI** received the bachelor's degree in electronic information engineering from the Chongqing University of Technology, Chongqing, China, in 2001, the master's degree in circuit and system from the University of Electronic Science and Technology of China, Chengdu, China, in 2004, and the Ph.D. degree in acoustics from Northwestern Polytechnical University, Xi'an, China, in 2015. He is currently an Associate Professor with the School of Electronic Engineering, Xi'an University of Posts and Telecommunications, Xi'an. His research interest includes underwater acoustic signal processing.

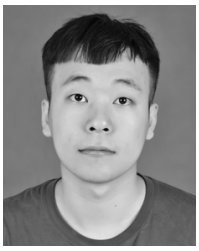

**JIUYANG CUI** received the bachelor's degree in electronic and information engineering from Zhengzhou Technology and Business University, Zhengzhou, China, in 2018. He is currently pursuing the master's degree in electronics and communication engineering with the Xi'an University of Posts and Telecommunications, Xi'an, China. His research interest includes underwater acoustic signal detection.

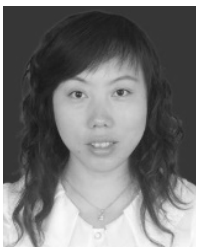

**HONG YANG** received the bachelor's and master's degrees in mechanical and electronic engineering from the University of Electronic Science and Technology of China, Chengdu, China, in 2003 and 2006, respectively, and the Ph.D. degree in acoustics from Northwestern Polytechnical University, Xi'an, China, in 2015. She is currently an Associate Professor with the School of Electronic Engineering, Xi'an University of Posts and Telecommunications, Xi'an. Her research interests include underwater acoustic signal processing and chaotic signal processing.